Hindawi Publishing Corporation
International Journal of Spectroscopy
Volume 2011, Article ID 458089, 8 pages
doi:10.1155/2011/458089

Research Article

In Situ IR Characterization of CO Interacting with Rh Nanoparticles Obtained by Calcination and Reduction of Hydrotalcite-Type Precursors

F. Basile,[1] I. Bersani,[1] P. Del Gallo,[2] S. Fiorilli,[3,4] G. Fornasari,[1] D. Gary,[2] R. Mortera,[3,4] B. Onida,[3,4] and A. Vaccari[1]

[1] *Dipartimento di Chimica Industriale e dei Materiali, Alma Mater Studiorum-Università di Bologna, V.le Risorgimento 4, 40136 Bologna, Italy*
[2] *Air Liquide, Centre de Recherche Claude Delorme1, Chemin de la Porte des Loges, BP 126, Les Loges-en-Josas, 78354 Jouy-en-Josas Cedex, France*
[3] *Dipartimento di Scienza dei Materiali e Ingegneria Chimica, Politecnico di Torino, Corso Duca degli Abruzzi 24, 10129 Torino, Italy*
[4] *CpR-INSTM for Materials with Controlled Porosity, Via Giusti 9, 50121 Firenze, Italy*

Correspondence should be addressed to B. Onida, barbara.onida@polito.it

Received 3 May 2011; Accepted 21 June 2011

Academic Editor: Sergio Armenta Estrela

Supported Rh nanoparticles obtained by reduction in hydrogen of severely calcined Rh/Mg/Al hydrotalcite-type (HT) phases have been characterized by FT-IR spectroscopy of adsorbed CO [both at room temperature (r.t.) and nominal liquid nitrogen temperature] and Transmission Electron Microscopy (TEM). The effect of reducing temperature has been investigated, showing that Rh crystal size increases from 1.4 nm to 1.8 nm when the reduction temperature increases from 750°C to 950°C. The crystal growth favours the formation of bridged CO species and linear monocarbonyl species with respect to *gem*-dicarbonyl species; when CO adsorbs at r.t., CO disproportionation occurs on Rh and it accompanies the formation of $Rh^{I}(CO)_2$. The role of interlayer anions in the HT precursors to affect the properties of the final materials has been also investigated considering samples prepared from silicate-instead of carbonate-containing precursors. In this case, formation of $Rh^{I}(CO)_2$ and CO disproportionation do not occur, and this evidence is discussed in terms of support effect.

1. Introduction

Hydrotalcites or layered double hydroxides (LDH's) belong to a large class of natural and synthetic anionic clays. Although they are less diffuse in nature than cationic clays, they can be easily synthesized [1]. Hydrotalcites-type (HT) compounds have the general formula:

$$\left[M^{2+}{}_{(1-x)}M^{3+}{}_{x}(OH)_2\right]^{b+}\left(A^{n-}{}_{b/n}\right)\, mH_2O \qquad (1)$$

The cations are present in a layer with brucite-type structure $[Mg(OH)_2]$, in which part of Mg^{2+} is replaced by Al^{3+} and, as a consequence, the positive additional charge of the cations is balanced by the insertion of anions between layers. Usually carbonates are used as anions, even if samples with silicates have shown higher thermal and textural stability [2].

The mixed oxides obtained after calcination of HT phases at temperature above 500°C are very useful for a wide range of applications like antiacids, anion exchanger, adsorbents, catalysts, and catalyst supports because of their undeniable advantages as high surface area and structural stability [3].

A further increase of the calcination temperature above 750°C gives rise to the segregation of the stoichiometric spinel phase and the formation of less defective MgO-type phase, giving rise to stable supports or catalysts for high temperature processes. In particular, the modification of the catalytic properties is possible by the substitution of part of Mg with other bivalent cation as Ni, Pt, Pd, Co, and/or

part of Al ions with Rh, Fe, Cr obtaining a high variety of formulation [3, 4].

The structure and surface properties of Mg-Al HT phases and of the resulting mixed oxides depend strongly on chemical composition and synthesis procedures [3].

Catalytic applications take advantage of their basic and/or redox properties, as the dispersion of the cations in the hydroxylated layers is retained after calcination, thus generating well-stabilized metallic particles. This property is particularly useful for catalysts active in H_2 production processes via reforming reactions. Considering that Rh is well known as one the most active metals for methane reforming, its insertion in the HT material leads to a very active catalyst with Rh particles highly dispersed on the surface of catalyst [5].

IR spectroscopy of adsorbed carbon monoxide has been widely used to characterize Rh-supported catalysts [6–11]. It is well known that three generalized types of chemisorbed CO are produced on dispersed Rh surfaces at room temperature, which are linear monocarbonyl species, $Rh^0(CO)$, bridging CO species, $Rh_2^0(CO)$, and *gem*-dicarbonyl complexes on oxidized Rh sites, $Rh^I(CO)_2$. The detection of the latter is considered significant for the existence of highly dispersed Rh, whereas linear and bridged carbonyl species are usually considered to form on extended Rh surface [6, 8, 10].

Besides giving information on dispersion of Rh, the study of interaction with CO allows to characterize the role of the support [7], which can strongly affect the catalytic activity [1]. Indeed, Rh in Rh/Mg/Al catalysts may be present in different phases. For instance, Rh/Mg/Al catalysts with high Rh content obtained by HT carbonate have been structurally characterised by sequential XRD and neutron diffraction Rietveld analysis, and Rh was shown to be present with a higher occupation factor inside the $MgAl_2O_4$ phase with respect to the MgO phase [12].

The aim of the work is twofold: on the one hand, the effect of the reducing treatment on Rh metal particles produced starting from Rh/Mg/Al HT precursors (1% by weight of rhodium) is investigated, analyzing two samples reduced at 750°C and at 950°C, respectively.

On the other hand, the effect of the support is investigated. To this purpose two materials with different M^{2+}/M^{3+} ratio and different anions between layers were taken in exam: one sample was prepared with carbonate and the ratio M^{2+}/M^{3+} was about 2, and the other one was prepared with silicate and the M^{2+}/M^{3+} ratio was 4. In fact, different anions give rise to different phases in the calcined system: for instance, upon calcination silicates react with part of magnesium to give forsterite-type phase [2].

The characterization of supported Rh particles has been carried out by means of interaction with CO both at room temperature (r.t.) and at nominal liquid N_2 temperature, being the reactivity of CO depending on temperature [6]. The study of adsorbed CO_2 has been also carried out in order to characterize products of CO reaction at room temperature.

IR spectroscopy data are discussed on the basis of X-ray diffraction and TEM characterization.

2. Experimental

2.1. Materials Preparation. Carbonate and silicate-containing HT precursors were synthesized by coprecipitation method at constant pH and temperature following the method previously reported [4]. A solution of nitrate salts was added drop by drop to a basic solution containing carbonate or silicate anions. pH was kept constant at 10.5 by dropwise NaOH addition. The obtained suspension was aged by stirring for 1 hour at 56°C, then filtered and washed with distilled water. The precipitate was dried overnight at 60°C and calcined at 900°C for 12 h.

Samples obtained from the carbonate solution (nominal composition $Rh_{0.43}Mg_{68}Al_{31.57}$) were reduced at 750°C for 2 h or at 950°C for 4 h under a 50 mL/min flow of an H_2-Ar mixture (3 : 97 v/v) and from now on will be named Rh/HTCarb_750 and Rh/HTCarb_950, respectively. The material obtained from the silicate solution (nominal composition $Rh_{0.5}Mg_{80}Al_{19.5}$) was reduced under a 50 mL/min flow of an H_2-Ar mixture (3 : 97 v/v) and will be named as Rh/HTSil_750.

2.2. Samples Characterization. XRD powder analyses were carried out using a Philips PW1050/81 diffractometer equipped with a graphite monochromator in the diffracted beam and controlled by a PW1710 unit (l = 0.15418 nm). A 2theta range from 5° to 80° was investigated at a scanning speed of 70°/h. In order to evaluate the particle size of phases, the silicon (plane (111)) was used to determine broadening of the X-ray reflections (FWHM). The calculation was performed with the X'Pert HighScore Program using the Scherrer's equation.

Transmission Electron Microscopy (TEM, JEOL 2010), combined with Energy Dispersive X-ray Spectrometry (EDS), was used to determine the size of the Rh particles in the samples reduced at different temperatures (according to that reported above) or obtained from carbonate- or silicate-containing HT precursors.

2.3. IR Study of Interaction with Probe Molecules. For IR, characterization powders were pressed into thin self-supporting pellets and then placed into a quartz IR cell. The activation treatment was carried out by connecting the cell to a vacuum-adsorption frame with a residual pressure below 10^{-3} mbar. In particular, prior to the adsorption measurements, all samples were activated by a treatment in H_2 (200 mbar) at 750°C (heating rate 2.5°C min^{-1}) for 1 h, outgassed under dynamic vacuum at 650°C for 2 h and then cooled to room temperature under Ar atmosphere.

FT-IR spectra were collected by using a Bruker Equinox 55 spectrometer, equipped with MCT cryodetector, at a spectral resolution of 2 $cm^{-1}$and accumulation of 32 scans. CO and CO_2 (from Messer) were dosed in the pressure range from 0.1 to 35 mbar by connecting the IR cell to a vacuum frame. The interaction with CO was studied both at r.t. and at the nominal temperature of −196°C by using liquid nitrogen as coolant. The actual temperature of the sample is about −173°C, due to the heating effect of the IR beam. Adsorption of CO_2 was studied at r.t.

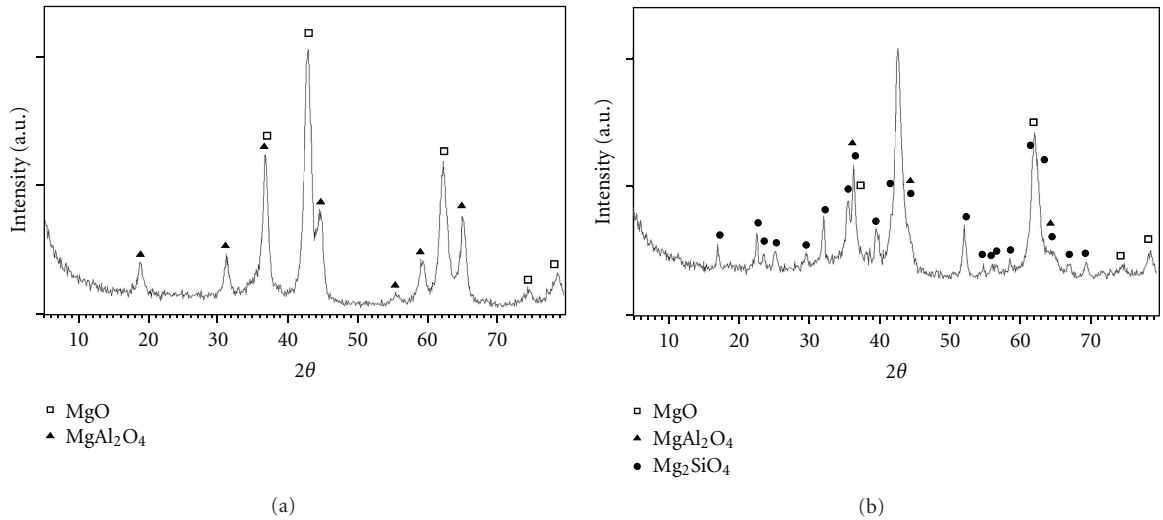

Figure 1: XRD patterns of Rh/HTCarb_750 (a) and Rh/HTSil_750 (b).

FT-IR spectra related to different samples were normalized dividing the registered intensities by the pellet weight (mg) and multiplying by the pellet area (mm^2). For this reason, absorbance is in arbitrary units (a.u.) and values are not reported in figures. All FT-IR spectra related to the dosage of CO and CO_2 are shown as difference spectra (the spectrum recorded before probe dosage was subtracted): positive bands indicate species which are formed during the *in situ* measurement, whereas negative bands, if present, are related to species which are consumed.

3. Results and Discussion

Rh/HTCarb_750 contains a spinel-type phase and a rock-salt-type phase, as revealed by the XRD pattern (Figure 1(a)).

The average particle sizes for MgO- and spinel-type phases, calculated by means of Sherrer's equation using the FWHM values of the most intense reflexions, are reported in Table 1. The average crystallite size of MgO-type phase in Rh/HT_Carb750 is close to 15 nm, while the spinel-type phase shows a slightly higher crystallite size (20 nm).

A complex pattern is observed for Rh/HTSil_750 (Figure 1(b)). Diffraction peaks assigned to a forsterite-like phase (Mg_2SiO_4) are indexed. Instead, no well-defined Al-containing phase ($MgAl_2O_4$) is detected [13]. In fact, only weak and broad reflections ascribable to a spinel-type phase are observed and the first two reflections at $2\theta = 19$ and 32°, ascribed to (111) and (220) planes, are not discernible in the pattern. This indicates that the silicates react with MgO to give the forsterite phase, affecting the formation of the spinel-type phase.

Since the MgO-type phase is the only phase observed in Rh/HTSil_750 also present in the Rh/HTCarb_750, the crystal size is estimated only for it and it appears larger than in the case of Rh/HTCarb 750.

For both Rh/HTCarb_750 and Rh/HTSil_750, no reflections due metallic Rh are observed, being its amount close to the instrumental detection limit.

Table 1: Crystal size of MgO- and $MgAl_2O_4$-type phases (nm) as obtained by XRD analysis.

Phase (*)	Rh/HTCarb_750	Rh/HTSil_750
MgO (200)	12	13
MgO (220)	15	17
MgO	13.5	15
$MgAl_2O_4$ (111)	18	/
$MgAl_2O_4$ (220)	34	/
$MgAl_2O_4$ (311)	24	/
$MgAl_2O_4$	25	/

(*)Reflections used for crystal size evaluation are reported.

Figure 2 reports the spectra related to increasing amount of CO adsorbed at r.t. on Rh/HTCarb_750 in the range 2200–1300 cm^{-1}. At very low CO pressure (spectrum 1), a single band is observed at 2050 cm^{-1}, assigned to the stretching mode of linear monocarbonyl species on Rh metal particles, $Rh^0(CO)$ [14, 15]. At increasing CO pressure, two shoulders appear above and below the band at 2050 cm^{-1}, due to, respectively, the symmetric and antisymmetric stretching modes of dicarbonyl species on oxidized Rh species, that is, $Rh^I(CO)_2$ [16]. In same spectra, absorptions below 1800 cm^{-1} increase, with maxima discernible at 1680 cm^{-1} and 1313 cm^{-1}, due to bidentate carbonates, at 1394 cm^{-1} and 1220 cm^{-1}, ascribed to hydrogenocarbonate-type and at 1380 cm^{-1}, assigned to formate-type species [17–19].

The spectrum recorded after removal of CO by outgassing at r.t. is reported in Figure 3 (curve 1). The band due to $Rh^0(CO)$ species is clearly observed at 2050 cm^{-1}. The weak band discernible at 2096 cm^{-1} is due to the symmetric stretching mode of $Rh^I(CO)2$ species. The twin antisymmetric mode, expected at around 2030 cm^{-1} [14–16], is most probably hidden in the tail of the main component at 2050 cm^{-1}, which indeed shows a low-frequency side asymmetry evidenced by the vertical broken line in the figure.

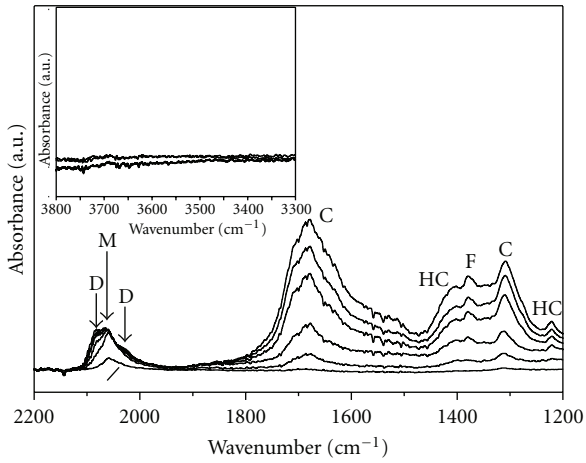

Figure 2: FT-IR spectra related to the adsorption of CO on Rh/HTCarb_750 at r.t. Section a: spectra recorded at increasing CO pressure. The inset shows the corresponding OH stretching region. Section b. Spectrum recorded after removal of CO from the IR cell at r.t. (D: *gem*-dicarbonyl, M: linear monocarbonyl, C: carbonate-, HC: hydrogenocarbonate-, and F: formate-type species).

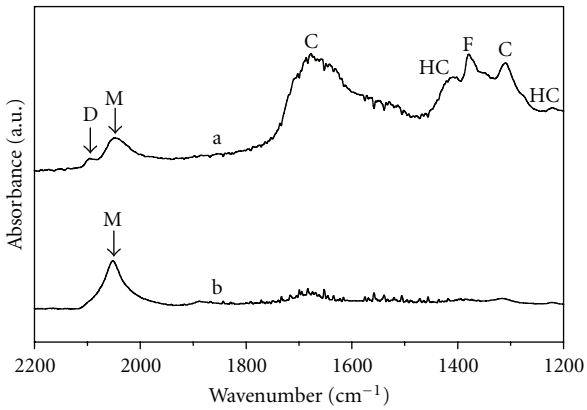

Figure 3: FT-IR spectra recorded after contact of CO with Rh/HTCarb_750 at r.t. (curve a) and at liquid N_2 temperature (curve b). (D: *gem*-dicarbonyl, M: linear monocarbonyl, C: carbonate-, HC: hydrogenocarbonate-, and F: formate-type species).

In the same spectra, bands due to carbonate-, hydrogenocarbonate-, and formate-type species are also observed.

As widely reported in the literature, species Rh^I are generally considered to form by reaction of CO on small Rh_x crystallites rather than present on the surface as such prior to contact with CO [10, 20, 21].

Indeed, the spectrum of CO adsorbed at low temperature (curve 2 in Figure 3) shows a single band at 2050 cm^{-1} due to linear monocarbonyl species on Rh^0. This suggests that species able to give *gem*-dicarbonyl species are not present on the surface, whereas they are formed by reaction with CO at room temperature.

The mechanism of formation of $Rh^I(CO)_2$ species upon reaction of CO is still under debate. It has been suggested that Rh-Rh bonds can be disrupted at r.t. and under CO pressure, due to the higher energy of the Rh-CO bond as compared

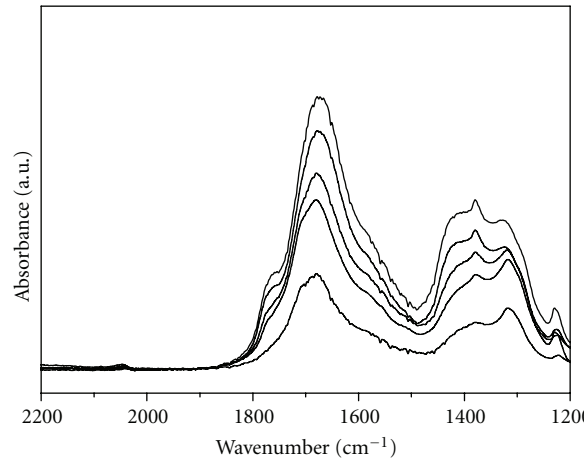

Figure 4: FT-IR spectra related to the adsorption of CO_2 on Rh/HTCarb_750 at r.t. (C: carbonate-, HC: hydrogenocarbonate-, and F: formate-type species).

to the Rh-Rh one [22], in small Rh_x particles. Some authors proposed that $Rh^I(CO)_2$ may form on two-dimensional Rh "islands" or Rh-isolated atoms [6, 23].

Primet [24] proposed that CO dissociation may occur even at −73°C on Rh, producing chemisorbed oxygen, leading to the formation of Rh^+ sites which are able to adsorb two CO molecules.

Moreover, the involvement of support OH species has been also proposed in a few cases [10, 25] according to the mechanism:

$$\left(\frac{1}{x}\right)Rh_x^0 + 2CO + OH^- \longrightarrow O^{2-} + Rh^+(CO)_2 + \frac{1}{2}H_2 \quad (2)$$

In the present case, the role of surface OH species, if any, is negligible, as revealed by the investigation of spectra in the OH stretching region (inset in Figure 2), where no significant modifications during reaction with CO are observed.

Despite the debate concerning the formation mechanism of $Rh^I(CO)_2$ species, however, the detection of *gem*-dicarbonyls is generally considered a strong indication of the existence of highly dispersed Rh metal particles on the catalyst surface.

In the present case, the formation of $Rh^I(CO)_2$ species is accompanied by the formation of carbonate-, hydrogenocarbonate-, and formate-type species, revealing that disproportionation of CO to C and CO_2 occurs. Indeed adsorption of CO_2 on the catalyst gives rise to similar absorption in the IR spectrum (Figure 4).

The reaction of CO occurs on Rh, since no formation of carbonate-type species has been observed for reaction of CO with the Rh-free support (spectra not reported). Disproportionation of CO on Rh supported on several oxides (TiO_2, Al_2O_3, SiO_2, MgO) has been reported in the literature, though at temperature higher than 25°C [7].

It is worth noting that in the spectrum of CO adsorbed at low temperature no bands due to carbonate-type species are observed, suggesting that carbonates form when $Rh^I(CO)_2$ species form. Indeed, though at temperature higher than

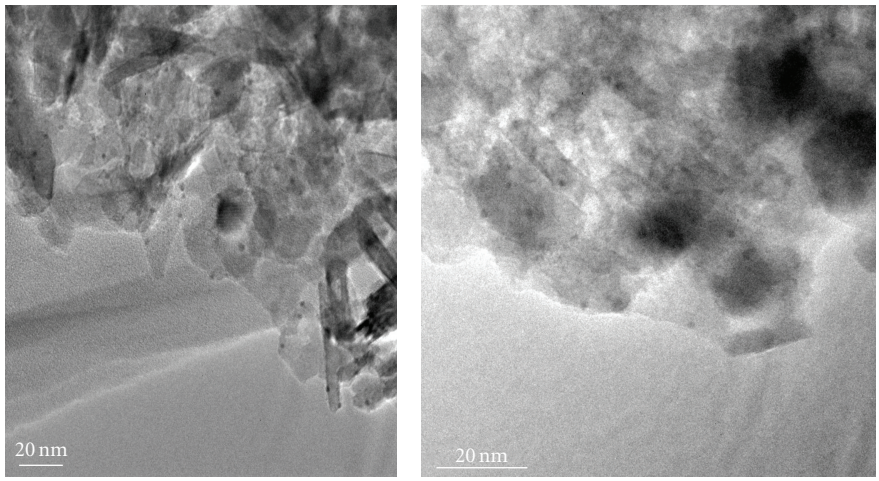

Figure 5: TEM micrographs of Rh/HTCarb_750 (upper part) and Rh/HTCarb_950 (lower part).

25°C, CO disproportionation on supported Rh was observed to occur with no evidence of presence of dicarbonyl species [7], some authors [26] suggested that the dissociation-disproportionation of CO should occur in the twin form in the case of Ru catalysts, which appears a reasonable mechanism, involving two CO molecules on the same metal site.

3.1. Effect of the Reducing Temperature. In order to investigate the effect of reducing temperature on the system, the sample reduced at 950°C (Rh/HTCarb_950) has been characterized following the same approach. The characterization has been completed by TEM analysis, and Figure 5 shows the TEM micrographs of Rh/HTCarb_750 and Rh/HTCarb_950. The Rh is in the form of well-dispersed nanoparticles in both cases. As expected, the average particle size appears smaller for the catalyst reduced at lower temperature (1.4 nm) than for that reduced at 950°C (1.8 nm).

Figure 6 shows the spectrum recorded after contact of Rh/HTcarb_950 with CO (p = 30 mbar) at r.t. and removal of the gas from the cell by outgassing. Spectra in presence of CO are similar and thus are not reported for sake of brevity.

The narrow band at 2060 cm^{-1} due to the $Rh^0(CO)$ species dominates the spectrum, whereas the symmetric mode of *gem*-dicarbonyl complexes appears as a shoulder at 2093 cm^{-1}, accompanied by the twin peak as a tail hardly discernible at about 2030 cm^{-1}. The relative intensity of the monocarbonyl band with respect to the symmetric *gem*-dicarbonyl mode is higher than for Rh/HTCarb_750, suggesting a larger population of the former species in the present case.

Moreover, a broad absorption is observed at about 1910 cm^{-1}, due to bridged-bonded carbonyl species, $Rh_2^0(CO)$ [25]. Both $Rh^0(CO)$ and $Rh_2^0(CO)$ arise from CO adsorbed on extended Rh faces. The lower amount of the former and the absence of the latter in Rh/HTCarb_750 are both in agreement with the existence of smaller Rh particles with respect to Rh/HTCarb_950, as revealed by TEM analysis. In particular, it may seem that the limit of average crystal size above which bridged-bonded carbonyl species are formed falls in the range of 1.4–1.8 nm.

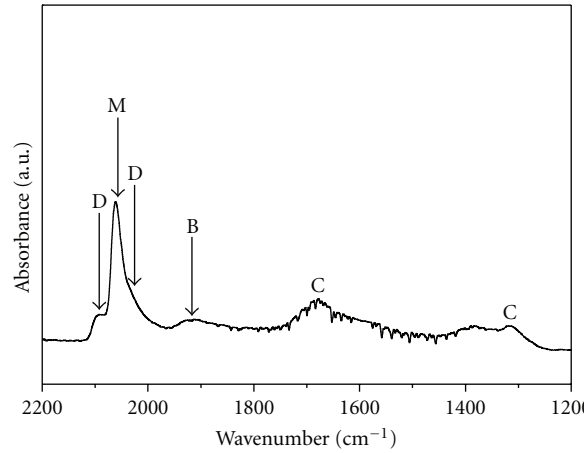

Figure 6: FT-IR spectrum recorded after contact of CO with Rh/HTCarb_950 at r.t. (D: *gem*-dicarbonyl, M: linear monocarbonyl, B: bridged-bonded CO, and C: carbonate-type species).

Though several authors reported the formation of bridged-bond $Rh_2(CO)$ upon adsorption of CO on supported Rh, very rarely information on particle size from complementary techniques is provided. Finocchio et al. [10] observed the occurrence of bridged-bond $Rh_2(CO)$ on particles with estimated size of 3.2 nm.

It is worth noting that in the case of Rh/HTcarb_950, only a very small amount of carbonate-like species are formed. The lower relative amount of $Rh^I(CO)_2$ in the present case suggests that formation of carbonate-type species is related to formation of *gem*-dicarbonyls upon reaction with CO. As observed for Rh/HTCarb_750, only monocarbonyl species are formed upon adsorption of CO at low temperature (spectrum not reported).

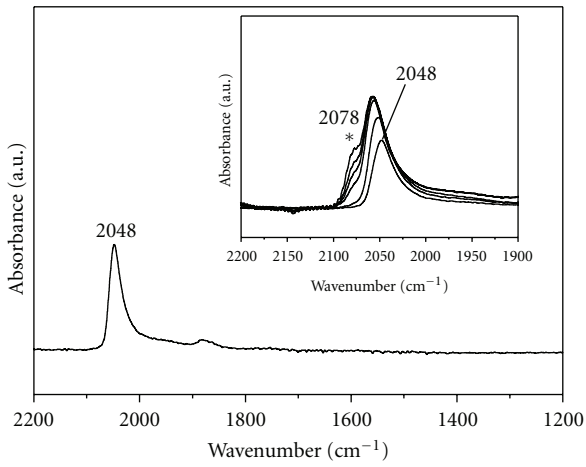

Figure 7: FT-IR spectrum recorded after contact of CO with Rh/HTSil_750 at r.t. Inset: spectra recorded at increasing CO pressure.

3.2. Role of the Support. The effect of the support has been investigated considering the reactivity of Rh/HTCarb_750 and Rh/HTSil_750 towards CO at r.t. Figure 7 reports the IR spectrum recorded after contact of Rh/HTSil_750 with CO (p = 30 mbar) at r.t. and removal of the gas from the IR cell by outgassing.

A single band is visible at 2048 cm^{-1}, due to monocarbonyl species on Rh surfaces. No bands due to *gem*-dicarbonyls are present, neither absorptions due to carbonate-type species. The results show that in Rh/HTSil_750 Rh is definitely less reactive towards CO with respect to Rh/HTCarb_750.

The lower reactivity cannot be ascribed to larger Rh particle size, that from TEM analysis (image not reported) shows a size of 1.1 nm, that is smaller than those observed on Rh/HTCarb_750.

An affect of the support may be instead envisaged, that may not favor the formation of $Rh^I(CO)_2$. The inset of Figure 7 reports the spectra recorded upon increasing CO pressure at r.t. Besides the shifting of the monocarbonyl band to higher frequency upon increasing coverage, due to dipole-dipole coupling among adsorbed CO molecules [10], a new component increases at 2078 cm^{-1} (labeled by an asterisk in figure). This absorption is depleted by outgassing at r.t., and in fact it is not visible in the spectrum reported in the main body of Figure 7, revealing that the related species is labile and adsorbed reversibly. We tentatively assign this band to monocarbonyl species on oxidized Rh, that is, $Rh^I(CO)$ species [15]. A similar species was proposed to account for a band observed at 2087 cm^{-1} on Rh/TiO_2 catalyst during decarbonylation [27]. These authors suggested that this species is an intermediate in the conversion of $Rh^I(CO)_2$ to $Rh^0(CO)$ and proposed that the corresponding band is frequently overlapped with the band above 2090 cm^{-1} due to *gem*-dicarbonyl species, so being indiscernible in most cases. The same band had been previously observed during initial adsorption of CO at low temperature on Rh/Al_2O_3 and it was assigned to Rh^I monocarbonyl species [28].

Assuming that the mechanism of decarbonylation is the reverse of the conversion of $Rh^0(CO)$ to $Rh^I(CO)_2$, we propose that the labile $Rh^I(CO)$ species forms at increasing CO coverage and it is a precursor of the *gem*-dicarbonyl species. It most probably forms also in the case of Rh/HTCarb_750 (Figure 2), being the band at 2078 cm^{-1} overlapped with the symmetric mode of the $Rh^I(CO)_2$, as previously suggested [19]. Indeed, upon CO removal (Figure 3) the high frequency shoulder of the monocarbonyl band at 2050 cm^{-1} is largely depleted, suggesting that species contributing to this adsorption are reversibly adsorbed.

Unlike the case of Rh/HTCarb_750, where *gem*-dicarbonyl forms, in the Rh/HTSil_750 the $Rh^I(CO)$ species do not evolve into $Rh^I(CO)_2$ complexes. A possible explanation is that $Rh^I(CO)_2$ species are not stabilized by the support. The role of the support in stabilizing $Rh^I(CO)_2$species was previously suggested [29]; for instance, it was reported that dicarbonyls are strongly favoured on Rh/Al_2O_3 compared to Rh/SiO_2 [8, 21].

Moreover, $Rh^I(CO)_2$ were observed to be dominant species on Rh/TiO_2 and Rh/Al_2O_3 reduced at 400°C, whereas this was not the case for Rh/SiO_2 and Rh/MgO reduced at the same temperature, mostly at low CO pressure [8].

Indeed, evidence of silicate forsterite-like phase (Mg_2SiO_4) is provided by XRD analysis, whereas no well-defined phase containing Al ($MgAl_2O_4$) is revealed, unlike Rh/HTCarb_750. Moreover, MgO crystals are more extended in Rh/HTSil_750 than in Rh/HTCarb_750.

It is worth noting that no carbonate-type species form on Rh/HTSil_750 upon interaction with CO, strongly suggesting, together with previous data, that $Rh^I(CO)_2$ are involved in CO disproportionation in these systems.

The lower reactivity in CO disproportionation of Rh/HTSil_750, containing the silicate forsterite-like phase (Mg_2SiO_4) instead of $MgAl_2O_4$, is in agreement with the observation that the extent of CO disproportionation on Rh catalyst follows the order Rh/Al_2O_3 > Rh/SiO_2 > Rh/MgO [8].

In conclusion, we propose that in Rh/HTCarb_750 Rh nanoparticles are affected by the Al-containing support, that is, the $MgAl_2O_4$ type phase in which the Rh has been reported to have larger solubility than for the MgO, when both phases are present [12]. Instead, in Rh/HTSil_750 the metal is affected mainly by MgO, acting as support.

Table 2 summarizes IR data related to CO adsorption, together with Rh particle size obtained by TEM data analysis.

4. Conclusions

Rh metal particles obtained by reduction in diluted H_2 of Rh/Mg/Al calcined HT precursors have been characterized by FT-IR analysis of adsorbed CO and TEM. The particle size increases from 1.4 nm to 1.8 nm when reduction temperature increases from 750°C to 950°C. The crystal growth causes, upon interaction with CO at r.t., the formation of bridged CO species and the increase of population of linear monocarbonyl in comparison to *gem*-dicarbonyl species.

Disproportionation of CO occurs on Rh at r.t., giving rise to carbonate-, hydrogenocarbonate- and formate-type species, and it accompanies the formation of $Rh^I(CO)_2$,

Table 2: FT-IR data of CO interaction at r.t. and Rh particle size evaluated by TEM analysis.

Sample	νRh^0CO (cm^{-1})	$\nu Rh^I(CO)_2$ (cm^{-1})	$\nu(Rh_2)CO$ (cm^{-1})	CO disprop.[c]	$d_{particles}$ (nm)
Rh/HTCarb_750	2050	2096[a]	—	YES	1.8
Rh/HTCarb_950	2060	2093, 2032[b]	1915	small extent	1.4
Rh/HTSil_750	2048	—	—	NO	1.1

[a]The asymmetric mode is overlapped with the monocarbonyl stretch.
[b]Lower relative amount with respect to Rh/HTCarb_750.
[c]CO disproportionation as revealed by the formation of carbonate-like species.

whereas no *gem*-dicarbonyl species and CO disproportionation are observed for reaction with CO at nominal liquid N_2 temperature.

The formation of $Rh^I(CO)_2$ and disproportionation of CO at r.t. do not occur for the sample obtained from the silicate-containing HT precursor. A band at 2078 cm^{-1} is ascribed to a labile $Rh^I(CO)$ species, which does not evolve into *gem*-dicarbonyl species. This is attributed to an effect of the support, which, at variance with the system prepared from carbonate solution, does not contain a well-defined spinel phase. Instead, it contains a silicate forsterite-like phase, besides the MgO phase which acts as support.

Acknowledgments

Thanks are due to INSTM Consortium and Air Liquide for the financial support. Special thanks are due to Professors T. Chartier and F. Rossignol (SPCTS, Limoges F) for the TEM images.

References

[1] S. Casenave, H. Martinez, C. Guimon et al., "Acid-base properties of Mg-Ni-Al mixed oxides using LDH as precursors," *Thermochimica Acta*, vol. 379, no. 1-2, pp. 85–93, 2001.

[2] S. Albertazzi, F. Basile, P. Benito et al., "Effect of silicates on the structure of Ni-containing catalysts obtained from hydrotalcite-type precursors," *Catalysis Today*, vol. 128, no. 3-4, pp. 258–263, 2007.

[3] F. Cavani, F. Trifirò, and A. Vaccari, "Hydrotalcite-type anionic clays: preparation, properties and applications," *Catalysis Today*, vol. 11, no. 2, pp. 173–301, 1991.

[4] F. Basile, P. Benito, G. Fornasari, and A. Vaccari, "Hydrotalcite-type precursors of active catalysts for hydrogen production," *Applied Clay Science*, vol. 48, no. 1-2, pp. 250–259, 2010.

[5] F. Basile, G. Fornasari, M. Gazzano, A. Kiennemann, and A. Vaccari, "Preparation and characterisation of a stable Rh catalyst for the partial oxidation of methane," *Journal of Catalysis*, vol. 217, no. 2, pp. 245–252, 2003.

[6] J. T. Yates Jr., T. M. Duncan, and R. W. Vaughan, "Infrared spectra of chemisorbed CO on Rh," *Journal of Chemical Physics*, vol. 71, 3908 pages, 1979.

[7] A. Erdöhelyi and F. Solymosi, "Effects of the support on the adsorption and dissociation of CO and on the reactivity of surface carbon on Rh catalysts," *Journal of Catalysis*, vol. 84, no. 2, pp. 446–460, 1983.

[8] S. Trautmann and M. Baerns, "Infrared Spectroscopic Studies of CO Adsorption on Rhodium Supported by SiO2, Al2O3, and TiO2," *Journal of Catalysis*, vol. 150, no. 2, pp. 335–344, 1994.

[9] L. Kundakovic, D. R. Mullins, and S. H. Overbury, "Adsorption and reaction of H2O and CO on oxidized and reduced Rh/CeOx(111) surfaces," *Surface Science*, vol. 457, no. 1, pp. 51–62, 2000.

[10] E. Finocchio, G. Buscai, P. Forzatti, G. Groppi, and A. Beretta, "State of supported rhodium nanoparticles for methane catalytic partial oxidation (CPO); FT-IR studies," *Langmuir*, vol. 23, no. 20, pp. 10419–10428, 2007.

[11] K. Hadjiivanov, E. Ivanova, L. Dimitrov, and H. Knözinger, "FTIR spectroscopic study of CO adsorption on Rh-ZSM-5: detection of Rh +-CO species," *Journal of Molecular Structure*, vol. 661-662, no. 1–3, pp. 459–463, 2003.

[12] F. Basile, G. Fornasari, M. Gazzano, and A. Vaccari, "Rh, Ru and Ir catalysts obtained by HT precursors: effect of the thermal evolution and composition on the material structure and use," *Journal of Materials Chemistry*, vol. 12, no. 11, pp. 3296–3303, 2002.

[13] F. Basile, P. Benito, G. Fornasari et al., "Ni-catalysts obtained from silicate intercalated HTlcs active in the catalytic partial oxidation of methane: influence of the silicate content," *Catalysis Today*, vol. 142, no. 1-2, pp. 78–84, 2009.

[14] T. Chafik, D. I. Kondarides, and X. E. Verykios, "Catalytic reduction of NO by CO over rhodium catalysts: 1. Adsorption and displacement characteristics Investigated by in situ FTIR and transient-MS techniques," *Journal of Catalysis*, vol. 190, no. 2, pp. 446–459, 2000.

[15] D. I. Kondarides, T. Chafik, and X. E. Verykios, "Catalytic reduction of NO by CO over Rhodium catalysts: 2. Effect of oxygen on the nature, population, and reactivity of surface species formed under reaction conditions," *Journal of Catalysis*, vol. 191, no. 1, pp. 147–164, 2000.

[16] H. Miessner, D. Gutschick, H. Ewald, and H. Müller, "The influence of support on the geminal dicarbonyl species RhI(CO)2 on supported rhodium catalysts: an IR spectroscopic study," *Journal of Molecular Catalysis*, vol. 36, no. 3, pp. 359–373, 1986.

[17] A. M. Turek, I. E. Wachs, and E. DeCanio, "Acidic properties of alumina-supported metal oxide catalysts: an infrared spectroscopy study," *Journal of Physical Chemistry*, vol. 96, no. 12, pp. 5000–5007, 1992.

[18] A. A. Davydov, M. L. Shepot'ko, and A. A. Budneva, "Study of the state of transition-metal cations on the catalyst surface by IR spectroscopy using adsorbed probe-molecules (CO, NO): X. Identification of the state of copper on the surface of Cu/SiO_2," *Kinetics and Catalysis*, vol. 35, p. 272, 1994.

[19] J. C. Lavalley, "Infrared spectrometric studies of the surface basicity of metal oxides and zeolites using adsorbed probe molecules," *Catalysis Today*, vol. 27, no. 3-4, pp. 377–401, 1996.

[20] G. Bergeret, P. Gallezot, P. Gelin et al., "CO-induced disintegration of rhodium aggregates supported in zeolites: in situ

synthesis of rhodium carbonyl clusters," *Journal of Catalysis*, vol. 104, no. 2, pp. 279–287, 1987.

[21] F. Solymosi, M. Pásztor, and G. Rákhely, "Infrared studies of the effects of promoters on CO-induced structural changes in Rh," *Journal of Catalysis*, vol. 110, no. 2, pp. 413–415, 1988.

[22] H. F. J. Van't Blik, J. B. A. D. Van Zon, T. Hulzinga, J. C. Vis, D. C. Koningsberger, and R. Prins, "An extended X-ray absorption fine structure spectroscopy study of a highly dispersed Rh/Al2O3 catalyst: the influence of CO chemisorption on the topology of rhodium," *Journal of Physical Chemistry*, vol. 87, no. 13, pp. 2264–2267, 1983.

[23] J. Raskó and J. Bontovics, "FTIR study of the rearrangement of adsorbed CO species on Al2O3-supported rhodium catalysts," *Catalysis Letters*, vol. 58, no. 1, pp. 27–32, 1999.

[24] M. Primet, "Infrared study of CO chemisorption on zeolite and alumina supported rhodium," *Journal of the Chemical Society, Faraday Transactions 1*, vol. 74, pp. 2570–2580, 1978.

[25] P. Basu, D. Panayotov, and J. T. Yates, "Rhodium-carbon monoxide surface chemistry: the involvement of surface hydroxyl groups on Al2O3 and SiO2 supports," *Journal of the American Chemical Society*, vol. 110, no. 7, pp. 2074–2081, 1988.

[26] A. Bossi, G. Carnisio, F. Garmassi, G. Giunchi, G. Petrini, and L. Zanderighi, "Isotopic equilibration of carbon monoxide catalyzed by supported ruthenium," *Journal of Catalysis*, vol. 65, p. 16, 1980.

[27] K. L. Zhang, A. Kladi, and X. E. Verykios, "Structural alterations of highly dispersed Rh/TiO2 catalyst upon CO adsorption and desorption investigated by infrared spectroscopy," *Journal of Molecular Catalysis*, vol. 89, no. 1-2, pp. 229–246, 1994.

[28] C. A. Rice, S. D. Worley, C. W. Curtis, J. A. Guin, and A. R. Tarrer, "The oxidation state of dispersed Rh on AI2O3," *The Journal of Chemical Physics*, vol. 74, no. 11, pp. 6487–6497, 1981.

[29] G. Lafaye, C. Mihut, C. Especel, P. Marécot, and M. D. Amiridis, "FTIR studies of CO adsorption on Rh-Ge/Al2O3 catalysts prepared by surface redox reactions," *Langmuir*, vol. 20, no. 24, pp. 10612–10616, 2004.